Robotica (2000) volume 18, pp. 639–649. Printed in the United Kingdom © 2000 Cambridge University Press

Optimal tripod turning gait generation for hexapod walking machines

S. Miao and D. Howard

Aeronautical & Mechanical Engineering, University of Salford, Salford, M5 4WT (UK)

(Received in Final Form: February 3, 2000)

SUMMARY

This paper describes an algorithm for generating a tripod turning gait which, when given an arbitrarily located turning centre, firstly maximises the rotation angle (angular stride) and then secondly optimises the stability. It does not require a specific walking machine layout or leg workspace shape, and it can deal with changes in the position of the CG caused by walking on a gradient or by uneven loading.

KEYWORDS: Hexapod walking machine; Gait study; Optimum stability; Gradient; Uneven loading.

1. INTRODUCTION

Gait study is a fundamental part of legged vehicle research. The first gait analyses were undertaken by zoologists investigating animal locomotion in the late nineteenth century. From the early 1960's, engineering scientists have been involved in gait study for the analysis, design and control of walking robots. McGhee and his co-workers developed the foundations for mathematical gait analysis based on the finite state concept and the static stability margin. They proposed the longitudinal stability margin to analyse the statically stable walking gaits of a quadruped.[1] Since then the longitudinal stability margin has been used as the main and often only performance criterion in gait studies.

Although a leg has only two simple states, leg on the ground denoted by 0 and leg in the air denoted by 1, it turns out that there are a huge number of theoretically possible gaits for a hexapod. But only a few of them have been observed in nature so far. One of the most common gaits used by insects and arthropod animals is the tripod gait.[2] It is regarded as the fastest gait for statically stable hexapods and is the simplest gait in terms of control. It has therefore often been adopted as the standard gait for hexapod walking machines.[3–5] Despite this, the analysis and optimisation of the tripod gait has not received as much attention as that of other forms of gait.

In previous studies, gait stability was usually the only performance criterion. Most researchers have been looking for maximum stability and basing their work on the assumptions that the machine's centre of gravity (CG) is coincident with the geometric centre of the body and that legs always pass through the centre of their workspace.[3–15] Thus the effective leg workspaces were straight lines or curves passing through the centres of the actual leg workspaces and parallel to the direction of motion. In addition, the walking machine model adopted has usually been based on a rectangular leg layout, with rectangular leg workspaces evenly spaced along two longitudinal axes which are equidistant from the machine's geometric centre. These assumptions have limited the performance of the gait algorithms developed, particularly in terms of stride length, stability, and the terrain that can be crossed.

The authors believe that gait stability should be a constraint, not an optimisation objective. It is proposed that the objective should be to maximise stride length (minimise the number of steps) given a required gait stability. Also, it is suggested that useful tripod gait algorithms should not be limited by the above assumptions, that is, the leg workspaces should be properly utilised, and algorithms must be able to cope with shifts in the vertical projection of the machine's CG caused by uneven loading or walking on uneven terrain.

From a theoretical point of view, turning gaits are the most general. Crab walking can be treated as a special case of turning when the turning centre is located at infinity, and longitudinal walking is a special case of crab walking when the crab angle is zero. Therefore, the objective of the study reported here was to develop an efficient algorithm for tripod turning which, when given an arbitrarily located turning centre, maximises rotation angle (angular stride) while guaranteeing the required stability margin. The proposed algorithm firstly maximises the rotation angle and then secondly optimises the stability. It does not require a specific walking machine layout or leg reachable workspace shape, and it can deal with changes in the position of the CG caused by walking up or down a slope, or by uneven loading.

This study assumes the general hexapod model shown in Figure 1. The legs are placed symmetrically about the longitudinal axis, but in all other respects the layout is completely general, being defined by P1, P2, W1, W2 and W3. The legs' reachable workspaces can be any shape so long as they can be approximated to straight sided polygons. During turning the body is kept at a constant height above the ground, so that the leg workspaces do not change.

Because the legs are symmetrical about the longitudinal axis, it is enough to demonstrate turning gait generation when the body rotates in one direction. Unless otherwise stated, the body rotates in the clockwise direction. Although the proposed algorithm has been designed for this general hexapod model, for convenience, the conventional rectangular layout is sometimes used as an example.

https://doi.org/10.1017/S0263574700002642 Published online by Cambridge University Press

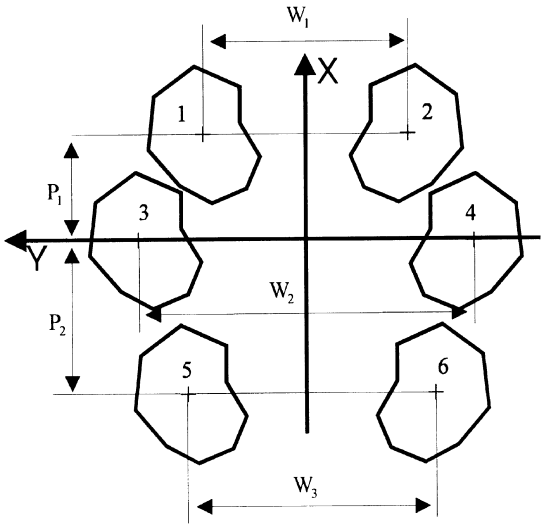


Fig. 1. A general model of a six legged walking machine.

2. GAIT STABILITY AND THE STABILITY CIRCLE

Most existing methods for determining the gait stability margin are based on the assumptions that the CG is coincident with the geometric centre of the body and that the legs pass through the centre of their workspaces.[3–15] Under these assumptions, it is sufficient to only calculate the stability margin at the critical events, namely immediately after a leg is lifted from the rear boundary of the support pattern and immediately before a leg is placed at the front boundary. In the more general case, minimum stability can occur at any instant during turning. Figure 2 shows an example where the middle of the CG's path is outside the support polygon.

In general, the stability margin has to be checked at every instant and the calculation of the minimum stability margin becomes more complicated. Therefore, the authors have developed a new method, referred to as the boundary angle method. This method can be used to determine:

- the stability margin at any position along the CG's path;
- the minimum stability margin and the position at which it occurs;
- and the segment of the path that violates the required stability margin.

A detailed description of the boundary angle method can be found in Dr Shan Miao's Ph.D. thesis.[16]

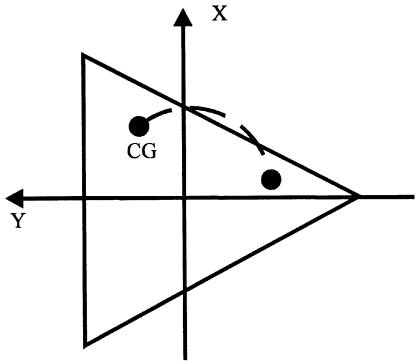


Fig. 2. Minimum stability can occur at any instant during turning.

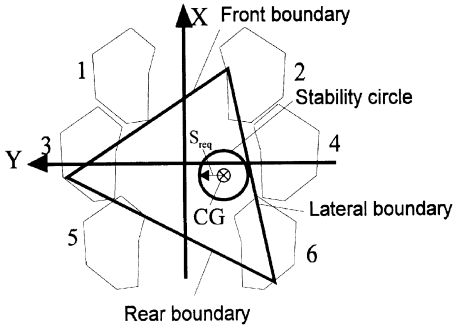


Fig. 3. Stability circle and support polygon boundaries.

2.1 The stability circle

Both the boundary angle method of gait stability calculation and the turning gait algorithm described here are based on the concept of the stability circle, which is defined as follows. The stability circle is a circle whose centre is coincident with the centre of gravity and whose radius equals the required minimum stability margin, S_{req}, as shown in Figure 3. During turning, none of the support polygon boundaries are allowed to cut into this circle.

3. THE TURNING GAIT GENERATION PROCEDURE

Referring to the objective of this study, mentioned in the introduction, the following problems were faced: (i) Each leg path generated must satisfy that leg's kinematic constraints; (ii) Each boundary generated must meet the minimum required stability margin; (iii) The tripod turning angle must be maximised, which is the primary criterion in this study; and (iv) The tripod's stability should be optimised, which is the secondary criterion.

Each tripod has its own maximum turning angle and three corresponding optimal leg paths. Thus the problem can be broken into 3 stages: (i) Find tripod A's maximum turning angle, Φ_A, and the corresponding leg paths; (ii) Find tripod B's maximum turning angle, Φ_B, and the corresponding leg paths; and (iii) Use this information to generate a continuous gait.

In the proposed procedure, the maximum possible tripod turning angle, Φ_A, neglecting static constraints, is found first and an approximate tripod, based on that Φ_A, is constructed. After the stability margin of each boundary has been checked, an optimisation procedure (the swing boundary procedure) is applied to alter the tripod to the optimal shape which possesses the maximum tripod turning angle and optimal stability.

If the minimum required stability is violated as a result of the swing boundary procedure, which means that Φ_A cannot be realised and needs to be reduced, the rolling boundary procedure is applied. The principle of this procedure is to roll the boundary around the stability circle, which guarantees the minimum required stability, to search for a new feasible maximum rotation angle.

3.1 The gait generation procedure

(i) For tripod A, eliminate the parts of the leg workspaces in which no leg path can be generated without

https://doi.org/10.1017/S0263574700002642 Published online by Cambridge University Press

violating the required stability. This is achieved by drawing a line which passes through one extreme corner of a leg workspace, and is tangential to the stability circle. If this line intersects the other leg workspace, then the part of the other leg's workspace which is on the same side of the line as the CG is eliminated. In Figure 4 the darkened areas are eliminated.

(ii) For tripod A, find each leg's $\Phi_{i\,max}$ and hence Φ_A. The path through a leg's workspace that maximises that leg's turning angle, about a given turning centre, can be found by comparing only those paths that pass through a vertex of the workspace or touch a boundary of the workspace.[16] After each leg's maximum turning angle, $\Phi_{i\,max}$, has been found, the maximum tripod turning angle can be determined. For tripods A and B the maximum turning angles are given by:

$$\Phi_A = \min(\Phi_{1\,max}, \Phi_{4\,max}, \Phi_{5\,max}),$$
$$\Phi_B = \min(\Phi_{2\,max}, \Phi_{3\,max}, \Phi_{6\,max})$$

This stage takes no account of stability constraints.

(iii) Construct initial tripod A, based on Φ_A. Once Φ_A is found, the corresponding leg's path is established. The other two leg paths can initially be chosen to be the segments of their current $\Phi_{i\,max}$ paths which maximise stability whilst corresponding to Φ_A. These will usually be the segment that is closest to: the top (bottom) boundary of leg 1's (5's) workspace; or the outer boundary of the middle leg's (leg 4's) workspace. Similar rules apply to tripod B (legs 2, 3 and 6).

Referring to Figure 5, leg 1 determined Φ_A, therefore, leg 1's path is also established. Leg 4 and 5's paths are the segments of the $\Phi_{4\,max}$ and $\Phi_{5\,max}$ paths which maximise stability. In both cases the approximate rules stated above apply.

Note that it is not a requirement of the method to place the paths of legs 4 and 5 in these positions, but the search range is significantly reduced if they are so placed.

(iv) Optimise stability (swing boundary procedure). After the initial stability margins have been determined, the stability is optimised using the swing boundary procedure. A full description of the procedure can be found in section 4. The result of this procedure is the final optimised tripod A, and the corresponding optimal leg paths. Ignore step 5, if the required minimum stability is not violated.

(v) Rolling boundary procedure. If the required minimum stability is violated at the end of the swing boundary procedure, the rolling boundary procedure is applied. The boundary that violated the stability circle is rolled around the stability circle, which guarantees the required minimum stability, to find a new feasible maximum rotation angle for the tripod. Section 5 describes the details of the procedure.

(vi) Repeat steps 1–5 for tripod B. The optimal tripod B can be found in exactly the same way as the optimal tripod A.

(vii) Generate continuous turning. When the optimal tripods A and B have been determined, continuous turning can be generated. The angular strokes associated with the two tripod supports must connect with each other. The position of the body's CG at the end of the first stroke is equal to its position at the start of the next stroke. No gap is allowed between two successive strokes. Successive tripod supports must be placed so that these rules are obeyed. A tripod is placed on the ground in the position, relative to the body, which corresponds to the start of its stroke. This occurs at the end of the previous stroke.

Figure 6 demonstrates continuous turning. Figure 6(a) and 6(b) show the motion of the optimal tripods, A and B respectively. Figure 6(c) shows the way these are combined to generate continuous turning. The CG starts at position 1 with tripod A beginning its support phase. The body rotates through an angle Φ_A and the CG reaches position 2. Position 2 is at the end of the first stroke which is also the start of the next stroke. The body then turns through an angle, Φ_B, and reaches position 3. Thus one turning cycle is completed. By repeating the same procedures, continuous turning is achieved.

4. THE SWING BOUNDARY PROCEDURE

The swing boundary method is a general method which can deal with problems where the maximum tripod turning angle is limited by kinematic constraints only, or by both

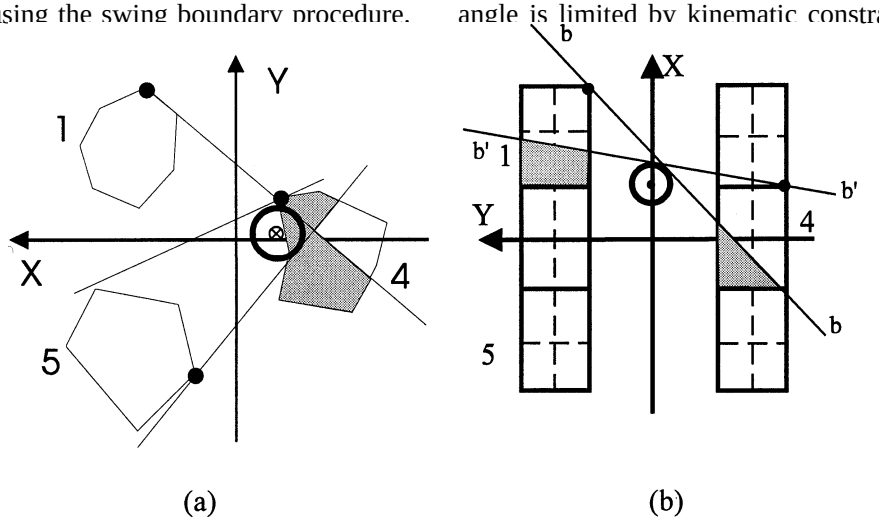


Fig. 4. Elimination of the unusable parts of the workspaces.

https://doi.org/10.1017/S0263574700002642 Published online by Cambridge University Press

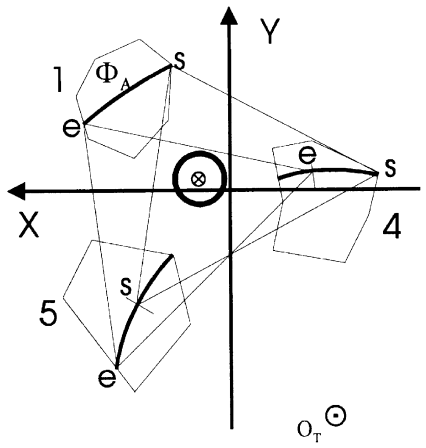


Fig. 5. Leg paths placement for initial tripod.

kinematic and static constraints. The optimisation procedure is based on the principle of making the three minimum stability margins as equal as possible while maintaining the maximum rotation angle. In practice, because of kinematic constraints and other limits, it is not always possible to make the three stability margins exactly equal. The optimisation is achieved by swinging two of the support polygon boundaries as close as possible to the desired equal stability margin positions whilst taking into account the third boundary's stability margin. After only a few iterations, the optimum tripod can be found. The following sections describe the details of the swing boundary procedure.

4.1 Definitions

Before describing the procedure, some definitions are needed:

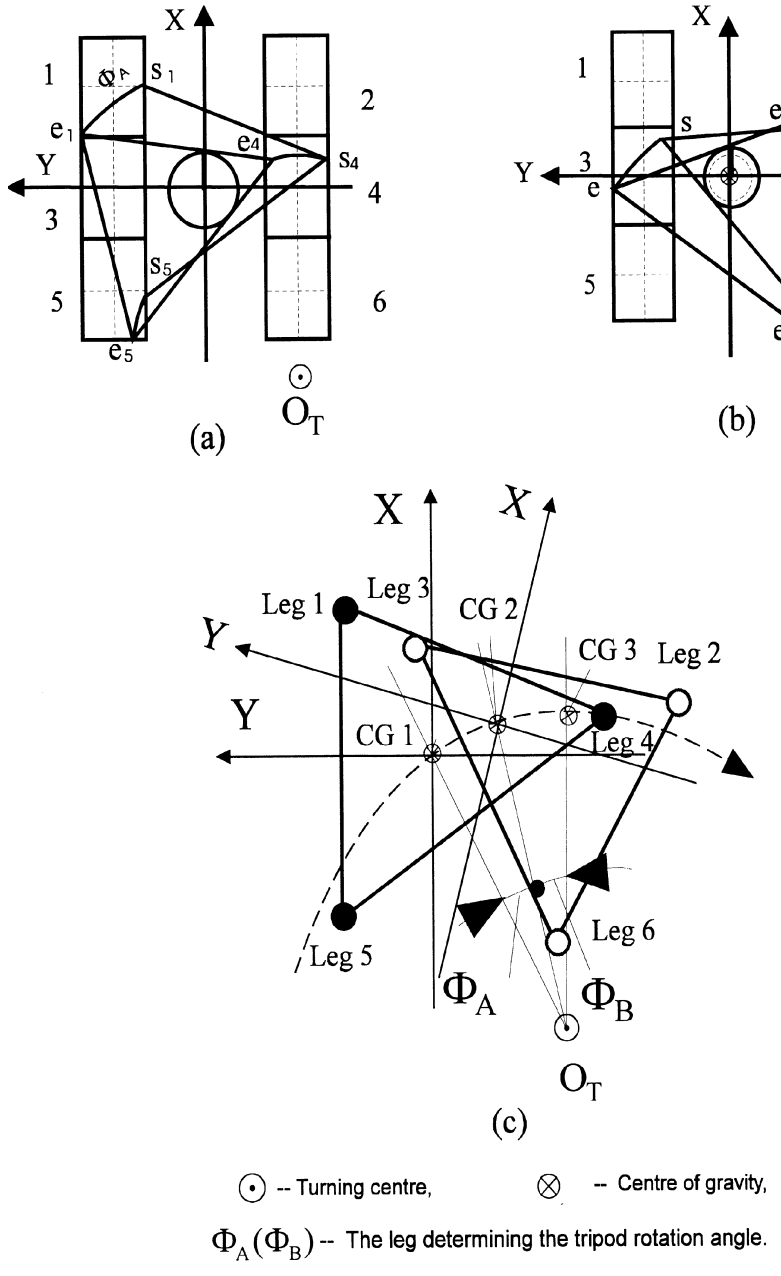


Fig. 6. Generating continuous turning.

https://doi.org/10.1017/S0263574700002642 Published online by Cambridge University Press

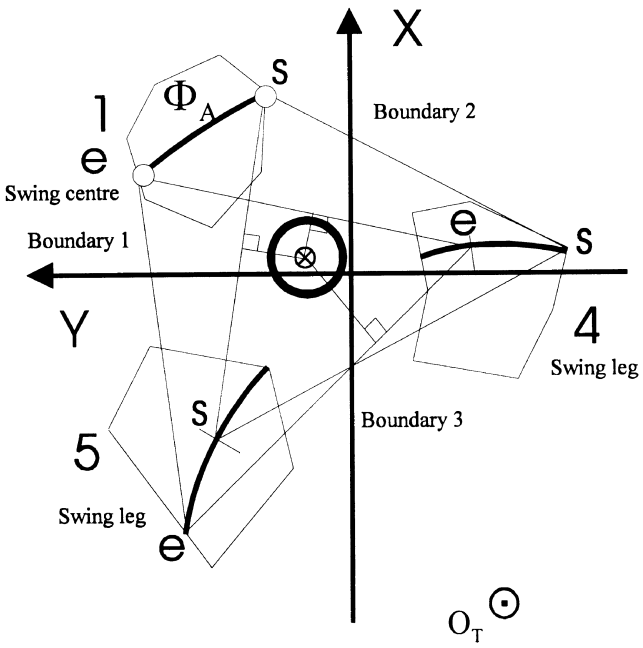


Fig. 7. Swing boundary and swing centre.

(a) *Boundary 1, 2 and 3* – Referring to Figure 7, the boundary which connects to the Φ_A leg and is on the left (right) side of the CG is defined as boundary 1 (2): the remaining boundary, which does not connect with the Φ_A leg, is boundary 3.

(b) *Swing boundary* – a boundary which is being swung (boundaries b_1 and b_2 in Figure 7).

(c) *Swing centre* – the leg about which the swing boundary is being swung. In other words, the end of the swing boundary that remains fixed (leg 1 in Figure 7). In this procedure, the swing centres are at the Φ_A or Φ_B leg. The position of the swing boundary at which the minimum stability margin occurs is used to define the swing centre. For example, because the minimum stability margin for boundary b_1 occurs at the start of its movement (**s**), its swing centre is leg 1 in its start position (**s**). Similarly, the swing centre for boundary b_2 is leg 1 in its end position (**e**).

(d) *Swing leg* – the leg at the other end of the swing boundary (legs 4 and 5 in Figure 7). In other words, the end of the swing boundary that rotates about the swing centre.

(e) *Swing angle* – The swing angle, α, is the angle formed by the swing boundary and the line which passes through the swing centre and the CG, as shown in Figure 8.

Referring to Figure 8, the relationship between the stability margin and the swing angle is:

$$S = D.\sin(\alpha) \quad (3)$$

$$\text{or } \alpha = \pm \sin^{-1}(S/D) \quad (4)$$

where: S is the stability margin, D is the distance between swing centre and CG, and α is the swing angle.

For a given swing centre, the maximum swing angle, α_{max}, and the minimum swing angle, α_{min}, of a swing boundary are determined by the corresponding swing leg's kinematic workspace. The two extremes of the swing leg workspace correspond to α_{max} and α_{min}, as shown in Figure 9 for leg 5.

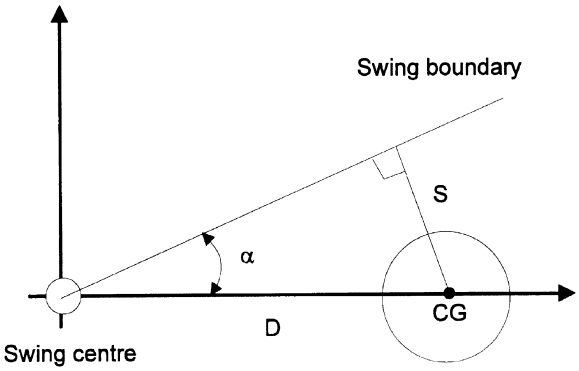


Fig. 8. The relationship between stability margin and swing angle.

4.2 The swing boundary procedure

The swing boundary procedure is presented in the flow chart shown in Figure 10, and each step described below.

(i) Calculate the minimum stability margin for each of the three boundaries and record the position of each boundary at which it occurs. Given an initial tripod, the minimum stability margin of each boundary, $S_{1\,min}$, $S_{2\,min}$ and $S_{3\,min}$, and the positions at which they occur can be determined using the boundary angle method.[16] The mean of the three minimum stability margins can be obtained thus:

$$\bar{S}_{min} = \frac{(S_{1\,min} + S_{2\,min} + S_{3\,min})}{3}$$

(ii) Set the target, S_T. The aim of the optimisation is to make the three minimum stability margins as equal as possible. The initial swing target is set to $S_T = \bar{S}_{min}$.

(iii) Establish initial swing angles. The initial swing angles for boundaries 1 and 2 are established as follows. According to equation 4, when given a target, S_T, the corresponding boundary swing angle, α_T, can be simply

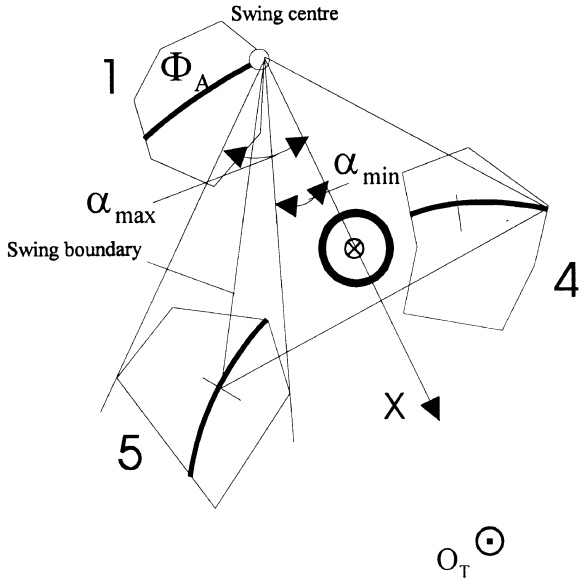


Fig. 9. The maximum and minimum swing angles.

https://doi.org/10.1017/S0263574700002642 Published online by Cambridge University Press

calculated. Taking into account kinematic limits, the swing angle, α, is the smaller (greater) of α_T and α_{max} (α_{min}), if the boundary is swung away from (towards) the CG. The swing direction depends upon the swing boundary's original S_{min} and S_T, in other words, the boundary is swung towards S_T from S_{min}.

(iv) Swing boundaries 1 and 2 about Φ_A leg. Boundaries 1 and 2 are swung to their new swing angles (α_1 and α_2) as defined in the previous step. They are swung about the Φ_A leg in their respective S_{min} positions.

(v) Establish leg paths. After swinging the boundaries, the swing leg paths are identified. Bear in mind that, during the swing boundary procedure the maximum rotation angle, Φ_A, should be maintained.

Each path must intersect with the corresponding swing boundary and the intersection point must correspond to the tripod position at which that boundary's stability margin was a minimum. For example, in Figure 11, the minimum stability margin, $S_{1\,min}$, occurred at the start of the tripod's movement, therefore, leg 5's new path must start from the new position of boundary 1.

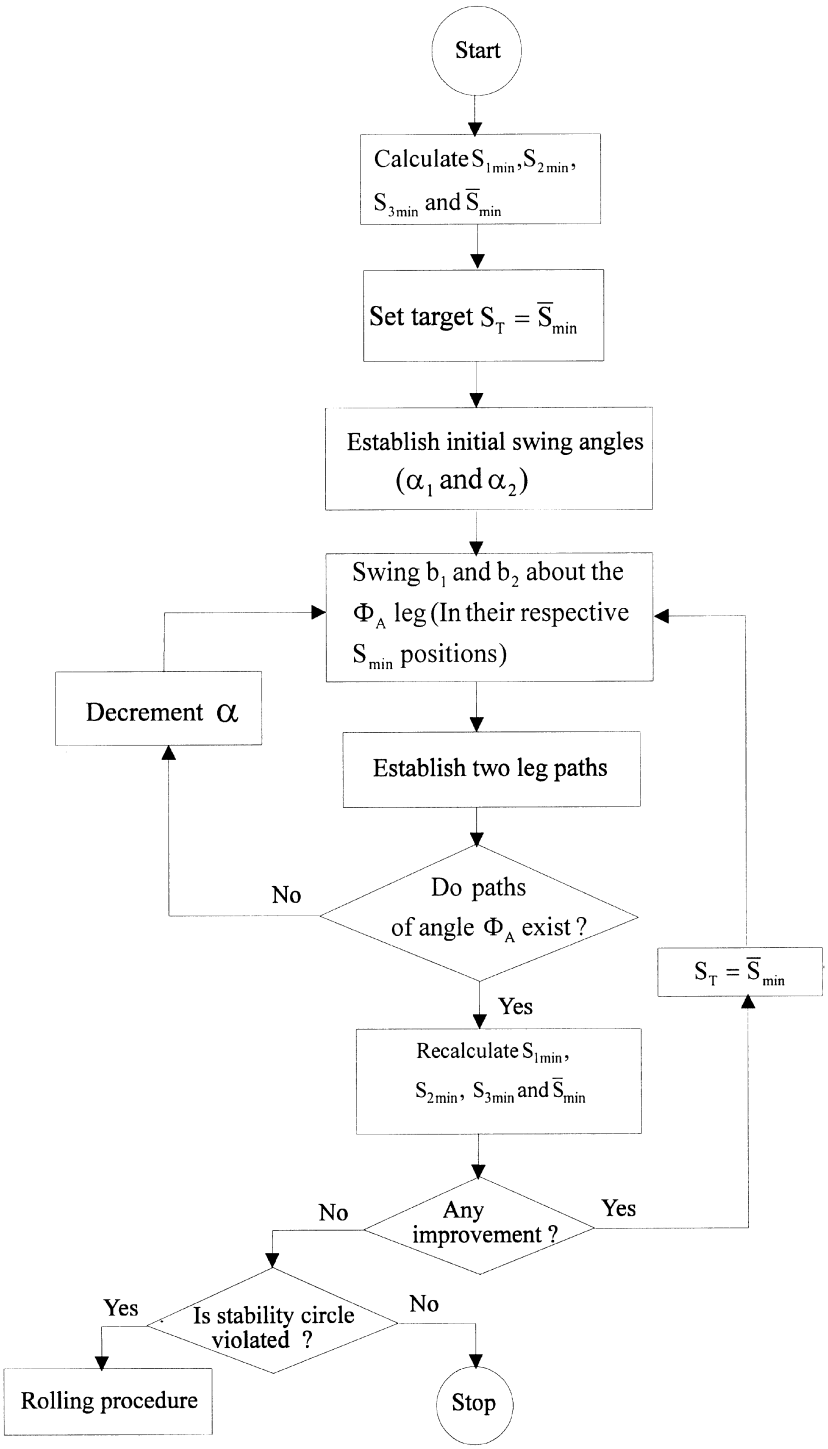


Fig. 10. Flow chart for the swing boundary procedure.

https://doi.org/10.1017/S0263574700002642 Published online by Cambridge University Press

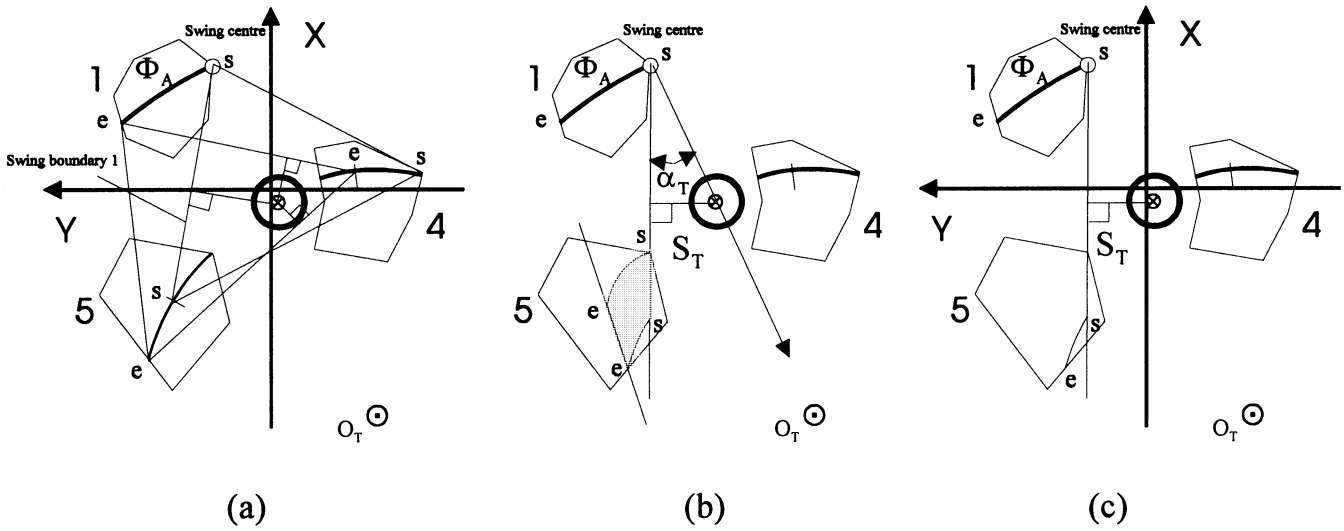


Fig. 11. Establishing a new swing leg path.

Property 1, described in the Appendix, can be used to find the family of paths, of angle Φ_A, that intersect with the new swing boundary at the correct point. Referring to Figure 11, boundary 1 is swung to the S_T position. Property 1, is used to determine the sector containing the family of Φ_A paths starting on boundary 1 (dotted area in Fig. 11(b)). The optimal path is the one furthest from the swing centre, because this maximises the stability margin of the third boundary (Fig. 11(c)).

Because of kinematic constraints or other limits, a path of angle Φ_A may not be found. In this case, the boundary has to be swung back towards its original position to find a feasible path. In other words, find a feasible swing angle, α_T, where a path of angle Φ_A exists. At each position, the same process for identifying a path, of angle Φ_A, is carried out. This continues until a feasible swing angle is found.

(vi) Recalculate three minimum stability margins and continue swing procedure. When the two new swing leg paths have been found, a new tripod can be constructed. The three minimum stability margins, $S_{1\,min}$, $S_{2\,min}$, $S_{3\,min}$ and $\bar{S}_{min}$ can be recalculated. If the minimum of $S_{1\,min}$, $S_{2\,min}$ and $S_{3\,min}$ has improved in the last iteration, the program adjusts target S_T and goes back to step 4 to continue the swing procedure. The new target, S_T, is given by:

$$S_T = \bar{S}_{min} \tag{5}$$

After only a few iterations, the optimal tripod will be found.

(vii) Check the minimum required stability margin. If the minimum stability margin (minimum of $S_{1\,min}$, $S_{2\,min}$ and $S_{3\,min}$) has not improved in the last iteration, then the tripod has been optimised (the swing boundary procedure has finished). In this case, the minimum stability margin is compared with the required minimum (S_{req}). If S_{req} is violated, the rolling boundary procedure is executed which is described in the following section.

4.3 An example of the swing boundary procedure

The initial tripod (Figure 12(a)) is determined prior to applying the swing boundary procedure, leg 3 is the Φ_B leg. The three minimum stability margins and the positions where they occur are determined using the boundary angle method.[16] The swing target, S_T, is set equal to the average of the three margins, $\bar{S}_{min}$. The corresponding swing angles for boundary 1 and 2 are determined, and the boundaries are swung, in this case, $\alpha_1 = \alpha_2 = \alpha_T$ (Fig. 12(b)). Figure 12(c) shows the result of the leg paths search, a sector containing the family of Φ_B paths at the α_T position of leg 6 was found. For leg 2, no path of angle Φ_B was found at the α_T position. Therefore, boundary b_2 had to be swung back, until a path of angle Φ_B was found. A new tripod is constructed and the minimum stability margins are recalculated as shown in Figure 12(d). The target is adjusted according to equation 5 and a second iteration is executed. Because boundary 2 is constrained by leg 2's kinematic workspace, there is no improvement in its minimum stability, $S_{2\,min}$. Therefore, after checking that S_{req} has been satisfied, the procedure is stopped. Figure 12(d) shows the optimal tripod.

5. THE ROLLING BOUNDARY PROCEDURE

If, at the end of the swing boundary procedure, the required minimum stability is violated, Φ_A cannot be realised and needs to be reduced. The objective in this case is to find a statically feasible maximum rotation angle, in other words, one which maintains the required minimum stability margin rather than optimising stability; this differs from the objective of the swing boundary procedure.

According to the stated aims of this study, Φ_A should not be reduced more than necessary, in other words, Φ_A should be reduced to just meet the required minimum stability. Furthermore, because we are dealing with a non-linear geometric problem, the necessary rotation angle reduction cannot be found in a closed form way. In order to efficiently find the new maximum Φ_A, the rolling boundary method is introduced. The maximum rotation angle is found by rolling the boundary that violated the stability circle around the stability circle, thus guaranteeing the required minimum

https://doi.org/10.1017/S0263574700002642 Published online by Cambridge University Press

stability (Fig. 13). The details of the procedure are as follows.

5.1 The rolling boundary procedure

(i) Establish initial rolling boundary position. The initial rolling boundary position is established by drawing a line which passes through one end of the boundary which violated the stability circle and is tangential to the stability circle (line rr in Fig. 14(b)). The rolling boundary represents the position of the boundary where its minimum stability margin originally occurred. For example, in Figure 14, boundary 3 violates the stability circle at the end of its path, therefore, the rolling boundary represents the end position of the boundary.

(ii) Determine the maximum rotation angles. At each rolling boundary position, the maximum rotation angles, $\Phi_{i\,max}$ and $\Phi_{j\,max}$, and the corresponding leg paths, for the two legs' which form the rolling boundary (leg 4 and 5 in Fig. 14), are established using a similar method to that used in step (ii) of the gait generation procedure (Section 3.1). The leg paths must include the rolling boundary and their intersection with the boundary must correspond to the tripod

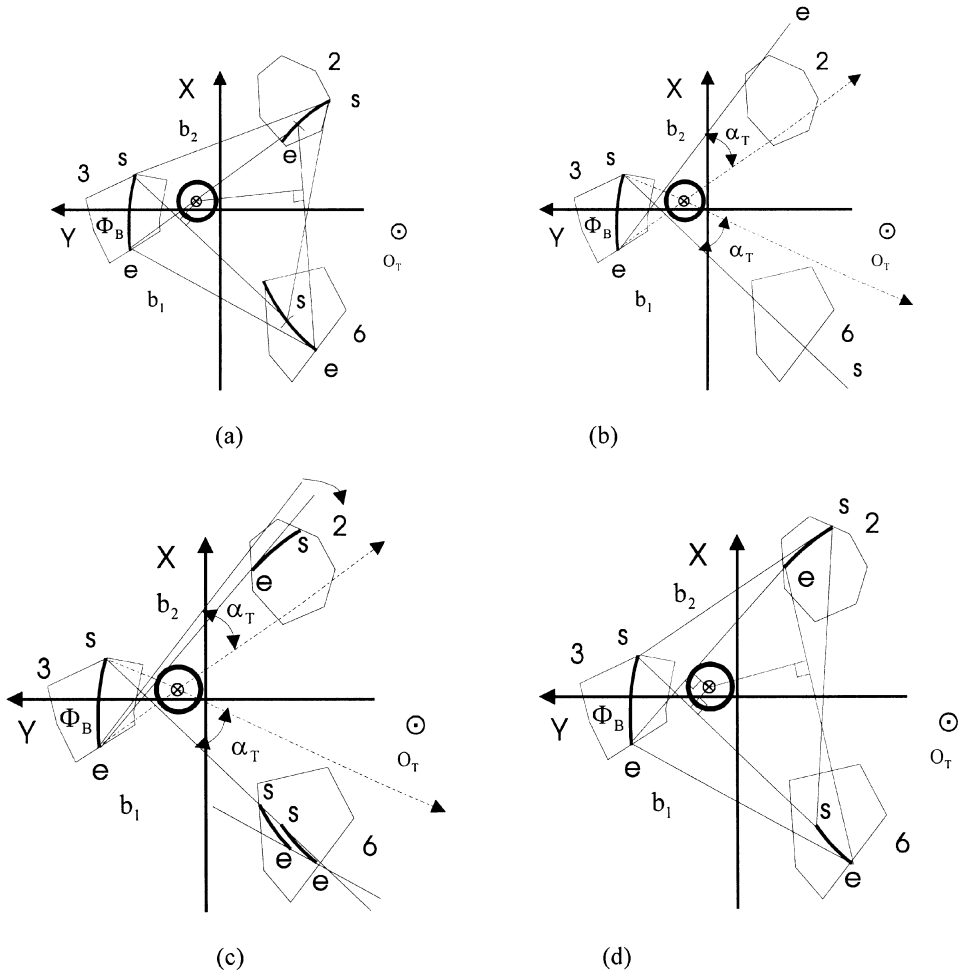


Fig. 12. An example of the swing boundary procedure.

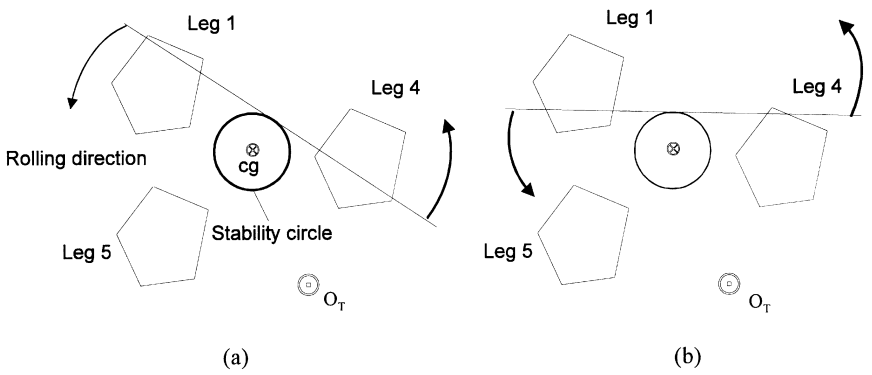


Fig. 13. Rolling boundary.

https://doi.org/10.1017/S0263574700002642 Published online by Cambridge University Press

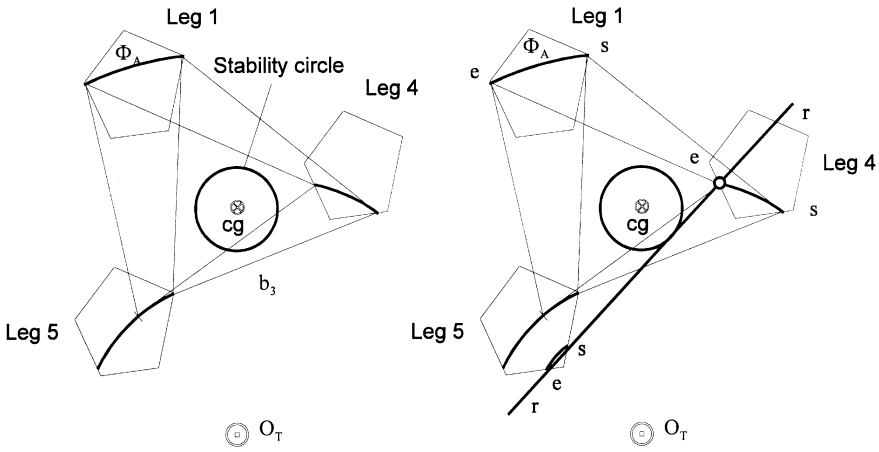


Fig. 14. Establish initial rolling boundary and the new path.

position at which the original boundary stability margin was a minimum, (Fig. 14(b)).

(iii) Compare the two maximum rotation angles. If the two maximum rotation angles, $\Phi_{i\,max}$ and $\Phi_{j\,max}$, are equal, within a suitable tolerance, then jump to step (v).

(iv) Roll the boundary. The boundary is rolled an increment around the stability circle and the procedure begins again from step (ii). The correct rolling direction is that which makes the two legs' maximum rotation angles converge.

(v) Determine the third leg path. This step is reached when the two maximum rotation angles have converged. In this case $\Phi_A = \Phi_{i\,max} = \Phi_{j\,max}$ and the third leg path is placed in a preferred position which allows a rotation of Φ_A. The preferred positions are those which are likely to improve other stability margins, i.e., the top (bottom) boundary of leg 1's (5's) workspace; or the outer boundary of the middle leg's (leg 4's) workspace.

(vi) Check the stability margin. If another boundary violates the required minimum stability, restart the procedure. Otherwise the procedure is complete.

5.2 An example of the rolling boundary procedure

Referring to Figure 15(a), the swing boundary procedure has been applied and boundary 2 violates the required stability margin, S_{req}. The swing process cannot be carried any further, and the rolling boundary method is applied. Figure 15(b) shows the initial rolling boundary position, which passes through the end of the leg 1 path and is tangential to the stability circle. The rolling direction is clockwise. In Figure 15(c), the position where $\Phi_{1\,max} = \Phi_{4\,max}$ is found. The new maximum rotation angle is $\Phi_A = \Phi_{1\,max} = \Phi_{4\,max}$. Leg 5's path is determined according to the new Φ_A and its preferred position, the bottom boundary of the workspace. The corresponding optimal tripod is shown in Figure 15(d).

6. CONCLUSIONS

A general algorithm for tripod turning gait generation has been developed. The method firstly maximises the rotation angle and then secondly optimises the stability. The proposed algorithm does not require a specific walking machine layout or leg reachable workspace shape. It can deal with changes in the position of the CG caused by walking up or down a slope, or by uneven loading.

The algorithm needs only a few iterations to find the optimal tripods. It covers "circling" gaits and "spinning" gaits, and therefore avoids the problems associated with clearly defining the two. The method has been tested graphically,[16] rather than by software implementation. This was because the focus of the work was on the development of new gait generation algorithms rather than their software implementation which would require the coding of a library of standard geometric algorithms.

Previously reported methods of calculating the minimum stability margin are not applicable to a general turning gait. This problem was solved by introducing a new method, the boundary angle method.[16] This method can simply indicate: whether a boundary violates the stability requirement or not; if it does, where it violates the stability requirement; in which position the minimum stability margin occurs; and the value of the stability margin at any position.

References

1. R.B. McGhee, "Finite state control of quadruped locomotion", *Mathematical BioSciences*, No. 13, 179–193, 1972.
2. D.M. Wilson, "Insect walking", *Ann. Rev. Entomol.*, **11**, 103–121 (1966).
3. I.E. Sutherland and M.K. Ullner, "Footprints in the asphalt", *Int. J. Robotics Res.*, **3**, No. 2, pp. 29–36, (1984).
4. M. Russell, "ODEX 1: The first functionoid", *Robotics Age*, **5**, No. 5,12–18 (1983).
5. R.B. McGhee and K.J. Waldron, "The adaptive suspension vehicle project: A case study in the development of an advanced concept for land locomotion", *Unmanned Systems*, **4**, No. 1, 34–43 (1985).
6. A.P. Bessonov and N.V. Umnov, "The analysis of gaits in six-legged vehicles according to their static stability", *Proc. Symp. Theory and Practice of Robots and Manipulators* Udine, Italy (1973) pp. 1–10.
7. S.M. Song and K.J. Waldron, "An analytical approach for gait study and its applications on wave gaits", *Int. J. Robotics Res.*, **6**, No. 2, 60–70 (Summer, 1987).
8. S.M. Song and B.S. Chio, "The optimally stable ranges of 2n-legged wave gaits", *IEEE Trans. Syst. Man Cyber.*, **20**, No. 4, 888–902 (Jul./Aug., 1990).

https://doi.org/10.1017/S0263574700002642 Published online by Cambridge University Press

9. D.E. Orin, "Supervisory control of a multilegged robot", *Int. J. Robotics Res.*, **1**, No. 1, 79–91, (Spring, 1982).
10. T.T. Lee, C.M. Liao and T.K. Chen, "On the stability properties of hexapod tripod gait", *IEEE J. Robotics and Automation*, **4**, No. 4, 427–434 (Aug., 1988).
11. S. Hirose, "A study of design and control of a quadruped walking vehicle", *Int. J. Robotics Res.*, **3**, No. 2, 113–133, 1984.
12. S. Hirose, H. Kikuchi and Y. Umetani, "The standard circular gait of a quadruped walking vehicle", *Adv. Robotics*, **1**, No. 2, 143–164 (1987).
13. C.D. Zhang and S.M. Song, "Gaits and geometry of a walking chair for the disabled", *J. of Terra Mechanics*, **26**, No. 3/4, 21–233 (1989).
14. Z. Bien, M.G. Chun and H.S. Son, "An optimal turning gait for a quadruped walking robot", *IEEE/RSJ Int. Workshop on Intelligent Robots and Systems IROS'91* Osaka, Japan, (1991) pp. 1511–1517.
15. C.D. Zhang and S.M. Song, "Turning gaits of a quadruped walking machine", *Proc. of IEEE International Conference on Robotics and Automation*, Sacramento, CA (April, 1991) **Vol 3**, pp. 2106–2112.
16. S. Miao, "Six legged walking machine gait and design", *Ph.D. thesis* (University of Salford, UK, 1998).

APPENDIX: PROPERTY 1

Property 1:
From an arbitrarily located turning centre, O_T, draw circles with different radii (Fig. 16). If any two arcs aa_1 and bb_1 defined by two lines, I and II, have the same rotation angle, $\Phi_1 = \Phi_2$, then any other arc defined by these two lines has an identical angle $\Phi = \Phi_1 = \Phi_2$.

Proof: In Figure 16, angle Φ_1 equals angle Φ_2, namely $\angle ao_Ta_1 = \angle bo_Tb_1$. In other words, two points on line I (a and b) have been rotated about O_T, through an angle $\Phi = \Phi_1 = \Phi_2$. This is a well known construction method for determining the new position of line I after it has been rotated through Φ about O_T. Therefore, line II is simply line I rotated through Φ and, hence, all points on that line have also been rotated through Φ. Therefore, any arc defined by lines I and II can be treated as a point on line I being rotated through an angle Φ.

Use of property 1: Property 1 can be used to establish the family of leg paths, of rotation angle Φ, that contact a boundary of the leg workspace. Figure 17(a) shows the family of leg paths that contact a boundary when the leg workspace and the turning centre, O_T, are on opposite sides of the boundary. Figure 17(b) shows the family of leg paths

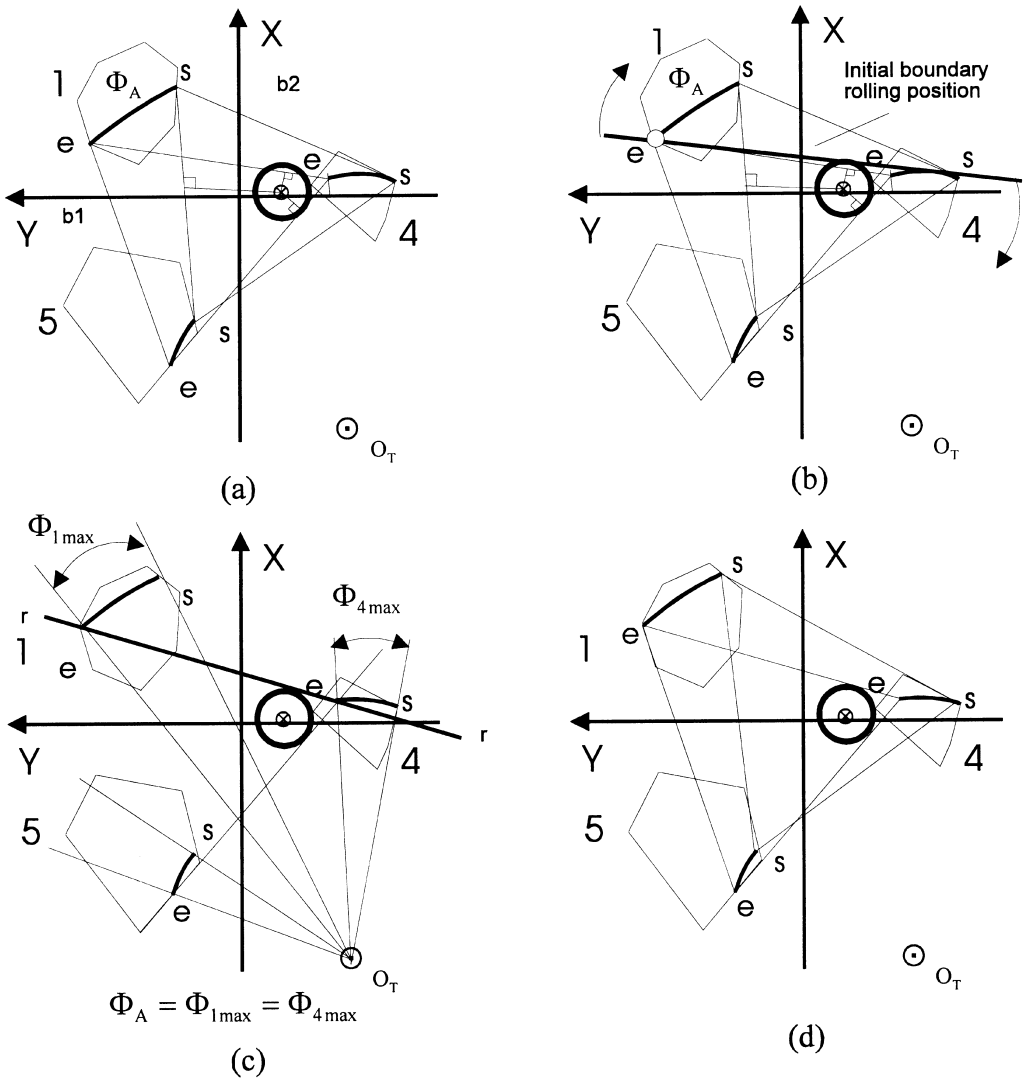


Fig. 15. An example of the rolling boundary method.

https://doi.org/10.1017/S0263574700002642 Published online by Cambridge University Press

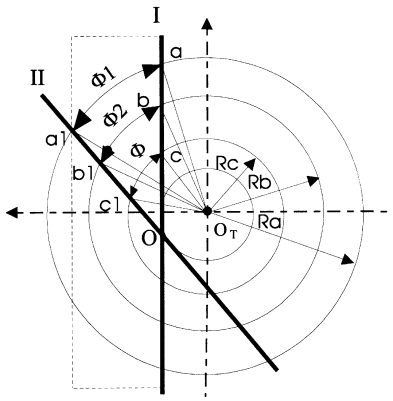


Fig. 16. Illustration of property 1.

that contact a boundary when the leg workspace and the turning centre are on the same side of the boundary. In Figure 17, it is assumed that the leg moves in an anti-clockwise manner, and hence, it is possible to identify the start and end lines.

In case 1 (Figure 17(a)), the start line, I, can be determined as follows: draw two arcs below O_T, about O_T, with identical rotation angle, Φ, and ending on the leg workspace boundary, (arcs s_4e_4 and s_5e_5). Draw a line which passes through the end points of the two arcs, s_4 and s_5, and intersects with the leg workspace boundary at s_3. This line together with the part of the boundary which is above the intersection point, s_3, forms the start line, I. The same method can be used to find the end line, II. Any leg paths defined by lines I and II and turning centre, O_T, have an identical rotation angle Φ, for example, paths s_1e_1, s_2e_2, s_4e_4 and s_5e_5.

In case 2 (Figure 17(b)), the start line, I, can be found as follows: draw two arcs above O_T, about O_T, with identical rotation angle, Φ, and ending on the workspace boundary, (arcs s_1e_1 and s_2e_2). Draw a line which passes through the end points of the two arcs, s_1 and s_2. Then draw the leg path which is tangential to the boundary (s_3e_3) and intersects with line s_1s_2 at s_3. The start line, I, is formed by three segments: the line s_1s_3; the part of the leg path , s_3e_3, between s_3 and the boundary; and the boundary below O_T, as shown in Fig. 17(b). The end line, II, can be found in a similar way. Again, any leg paths defined by lines I and II and turning centre, O_T, have an identical rotation angle Φ.

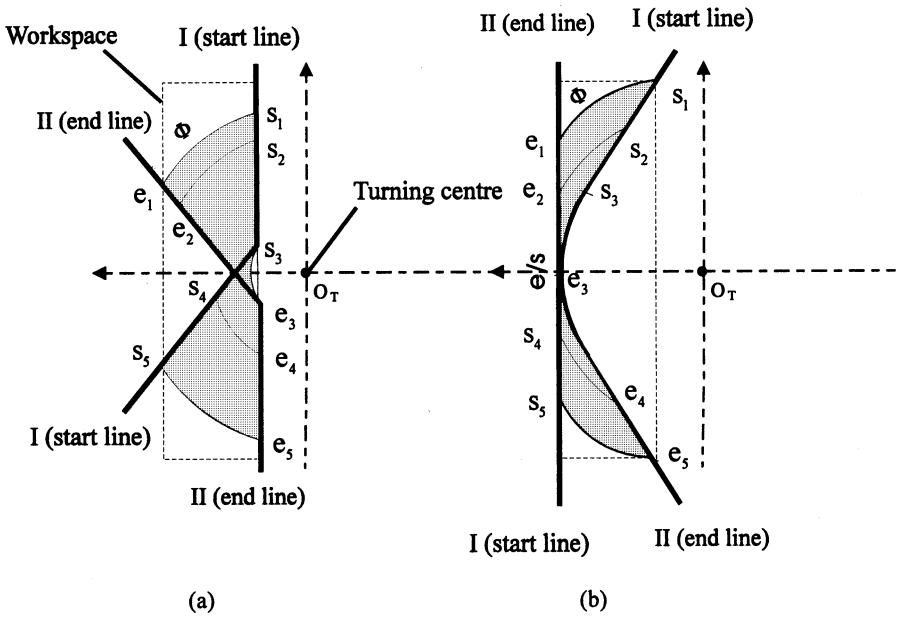


Fig. 17. The family of leg paths, of rotation angle Φ, that contact a boundary.
(a) case 1, (b) case 2.

https://doi.org/10.1017/S0263574700002642 Published online by Cambridge University Press